

1N-33
189389
21P

Solar Radiation on Mars: Stationary Photovoltaic Array

J. Appelbaum
National Aeronautics and Space Administration
Lewis Research Center
Cleveland, Ohio

I. Sherman
Tel Aviv University
Ramat Aviv, Israel

and

G.A. Landis
Sverdrup Technology, Inc.
Lewis Research Center Group
Brook Park, Ohio

October 1993

(NASA-TM-106321) SOLAR RADIATION
ON MARS: STATIONARY PHOTOVOLTAIC
ARRAY (NASA) 21 p

N94-14730

Unclas

G3/33 0189389

NASA



SOLAR RADIATION ON MARS: STATIONARY PHOTOVOLTAIC ARRAY

J. Appelbaum^{*}

National Aeronautics and Space Administration
Lewis Research Center
Cleveland, Ohio 44135

I. Sherman

Faculty of Engineering
Tel Aviv University
Ramat Aviv 69978, Israel

and

G.A. Landis^{**}

Sverdrup Technology, Inc.
Lewis Research Center Group
Brook Park, Ohio 44142

ABSTRACT

Solar energy is likely to be an important power source for surface-based operation on Mars. Photovoltaic cells offer many advantages. In this article we have presented analytical expressions and solar radiation data for stationary flat surfaces (horizontal and inclined) as a function of latitude, season and atmospheric dust load (optical depth). The diffuse component of the solar radiation on Mars can be significant, thus greatly affecting the optimal inclination angle of the photovoltaic surface.

1. INTRODUCTION

Missions to the Mars surface will most likely require electric power. Of the several possibilities, photovoltaic (PV) power systems can offer many advantages, including high power to weight ratio, modularity, and scalability. To design a photovoltaic system, detailed information on solar radiation data on the Martian surface is necessary. The variation of the solar radiation on the Martian surface is governed by three factors: (a) the variation in Mars-Sun distance, (b) variation in solar zenith angle due

^{*}Current address: Tel Aviv University, Faculty of Engineering, Tel Aviv, Israel. This work was done while the author was a National Research Council NASA Research Associate at NASA Lewis Research Center. Work was funded under NASA Grant NAGW-2022.

^{**}Sverdrup Technology, Inc. work was funded under NASA contract NAS-33-25266.

to Martian season and time of day, and (c) opacity of the Martian atmosphere. A Mars model for solar radiation was developed and published in Ref. [1].

A solar cell array mechanism may either be stationary or tracking. There are various configurations a stationary array (surface) may have. It may be horizontal, inclined with respect to ground, vertical, flat or curved; oriented toward the equator, toward East or any azimuth. A tracking array may track in two axes or in single axis of different kinds. This article deals with the solar radiation calculation on flat stationary surfaces on the surface of Mars. The solar radiation includes direct beam, diffuse and albedo. Optimal inclination angles for clear and cloudy skies are derived and the corresponding irradiances and insulations are calculated.

The calculation of solar radiation reaching a surface involves trigonometric relationships between the position of the Sun in the sky and the surface coordinates. The solar calculation expressions are in general form and pertain to Mars as well as to the Earth. The global irradiance G , in W/m^2 , on a surface is the sum of the direct beam irradiance G_b , the diffuse irradiance G_d , and the irradiance due to albedo G_{al} :

$$G = G_b + G_d + G_{al} \quad (1)$$

For a horizontal surface $G_{al} = 0$ and the irradiance is:

$$G_h = G_{bh} + G_{dh} \quad (2)$$

where:

G_h global irradiance on a horizontal surface

G_{bh} direct beam irradiance on a horizontal surface

G_{dh} diffuse irradiance on a horizontal surface

The global irradiance G_β on an inclined surface with an angle β , is:

$$G_\beta = G_b \cos \theta + G_{dh} \cos^2(\beta/2) + al G_h \sin^2(\beta/2) \quad (3)$$

where:

θ Sun angle of incidence, the angle between the beam irradiance on the surface and the normal to that surface

al albedo

As shown by Eq. (3), the irradiance on a surface is a function of the Sun incidence angle θ and the surface inclination angle β . These two angles will be determined for all types of stationary surfaces.

The surface optimal tilt angle for clear skies may be determined based on the maximum beam irradiance or maximum daily beam insolation. The surface optimal tilt angle for days with appreciable diffuse irradiance ("cloudy" skies) may be determined based on the maximum daily global insolation.

2. ANGLES INVOLVED IN SOLAR CALCULATION

2.1 Position of the Sun on a Horizontal Surface

The angles involved in the position of the Sun in the sky are shown in Fig. 1 [2]:

where:

z zenith angle

α solar altitude (or solar elevation); $\alpha = 90 - z$

ω hour angle; noon zero, morning negative, afternoon positive

T solar time; in hours (measured from midnight)

γ_s solar azimuth; south zero, east negative, west positive

The Mars day is 40 min, or about 2.75 percent, longer than a terrestrial day. Hence, when expressed in terms of standard (terrestrial) hours, the relation between actual time T and hour angle ω is slightly different for Mars than for Earth.¹ As shown in Fig. 2, the time (in terrestrial hours) and the hour angle ω are related by:

$$\text{Earth:} \quad \omega = 15T - 180 \quad (4A)$$

$$\text{Mars:} \quad \omega = 14.6T - 180 \quad (4B)$$

¹In some earlier papers [1], we have, for simplicity, expressed these equations in terms of "Mars hours" (H), defined by analogy to terrestrial hours (hr) as $24 H = 1 \text{ sol}$. Thus, one Mars hour = 1.0275 hr. In order that insolation values in kilowatt-hours to be expressed directly in terms of terrestrial hours, we have chosen here to use terrestrial hours rather than Mars hours. If the reader prefers to calculate in terms of Mars hours (i.e., Mars Mean Solar Time), the relationship between hour angle and solar time is identical to that for Earth.

The solar zenith angle is given by:

$$\sin \alpha = \cos z = \sin \phi \sin \delta + \cos \phi \cos \delta \cos \omega \quad (5)$$

where:

ϕ geographic latitude; north positive, south negative

δ declination, the angular position of the Sun at solar noon with respect to the plane of the equator; for Earth $-23.45^\circ \leq \delta \leq 23.45^\circ$, $\delta = 0^\circ$ at vernal and autumnal equinoxes, $\delta = +23.45^\circ$ at summer solstice and -23.45° at winter solstice. For Mars: $-24.936^\circ \leq \delta \leq 24.936^\circ$.

The solar azimuth angle is related by:

$$\cos \gamma_s = \frac{\sin \phi \cos \delta \cos \omega - \cos \phi \sin \delta}{\sin z} \quad (6)$$

or

$$\cos \gamma_s = \frac{\sin \phi \cos z - \sin \delta}{\cos \phi \sin z} \quad (7)$$

The sunrise and sunset hour angles are, respectively:

$$\omega_{sr} = -\cos^{-1}(-\tan \delta \tan \phi) \quad (8)$$

$$\omega_{ss} = \cos^{-1}(-\tan \delta \tan \phi) \quad (9)$$

for $|\phi| < \pi/2 - |\delta|$.

If $-\tan \delta \tan \phi > +1$ ($\phi < -\pi/2 + \delta$ or $\phi > \pi/2 + \delta$), the Sun will never rise nor set for the day: polar night.

If $-\tan \delta \tan \phi = \pm 1$, the Sun will be on the horizon for an instant only.

If $-\tan \delta \tan \phi < -1$ ($\phi > \pi/2 - \delta$ or $\phi < -\pi/2 - \delta$), the Sun will neither rise nor set for the day: polar day.

At the equator, $\phi = 0$; therefore $\omega_{sr} = \pi/2$, and the day length is independent of the solar declination (or season) and is always equal to 12 hr (on Earth), or 12.33 hr (on Mars).

At the equinoxes, $\delta = 0$; therefore $\omega_{sr} = \pi/2$, and the day length is independent of latitude and is equal to 12 hr (Earth), or 12.33 hr (Mars).

The sunrise and sunset azimuth angles are respectively:

$$\sin \gamma_{sr} = \cos \delta \cos \omega_{sr} \quad (10)$$

$$\sin \gamma_{ss} = \cos \delta \cos \omega_{ss} \quad (11)$$

and the number of daylight hours is:

$$\text{Earth:} \quad T_d = 2/15 \cos^{-1}(-\tan \delta \tan \phi) \quad (12A)$$

$$\text{Mars:} \quad T_d = 0.137 \cos^{-1}(-\tan \delta \tan \phi) \quad (12B)$$

2.2 Solar Angles of an Inclined Surface

The solar angles involved on an inclined surface are shown in Fig. 3, where:

β inclination, the angle between the surface and the horizontal

γ_c surface azimuth angle, the angle of the projection on a horizontal plane of the normal to the surface from the local meridian; zero south, east negative, west positive, $-180^\circ \leq \gamma_c \leq 180^\circ$, Fig. 4.

The Sun angle of incidence on a surface in terms of the Sun and surface angles is given by:

$$\cos \theta = \cos \beta \cos z + \sin \beta \sin z \cos(\gamma_s - \gamma_c) \quad (13)$$

or

$$\begin{aligned} \cos \theta &= \sin \delta \sin \phi \cos \beta - \sin \delta \cos \phi \sin \beta \cos \gamma_c \\ &+ \cos \delta \cos \phi \cos \beta \cos \omega + \cos \delta \sin \phi \sin \beta \cos \gamma_s \cos \omega \\ &+ \cos \delta \sin \beta \sin \gamma_c \cos \omega \end{aligned} \quad (14)$$

The sunrise ω_{cr} and sunset ω_{cs} hour angles on an inclined surface that is oriented toward the east, $\gamma_c < 0$,

Fig. 4, is given by:

$$\omega_{cr} = -\min \left[|\omega_{sr}|, \cos^{-1} \left(\frac{-xy - \sqrt{x^2 - y^2 + 1}}{x^2 + 1} \right) \right] \quad (15)$$

$$\omega_{cs} = \min \left[\omega_{ss}, \cos^{-1} \left(\frac{-xy + \sqrt{x^2 - y^2 + 1}}{x^2 + 1} \right) \right] \quad (16)$$

and for a surface that is oriented toward the west, $\gamma_c > 0$, Fig. 4, the angles are:

$$\omega_{cr} = -\min \left[|\omega_{sr}|, \cos^{-1} \left(\frac{-xy + \sqrt{x^2 - y^2 + 1}}{x^2 + 1} \right) \right] \quad (17)$$

$$\omega_{cs} = \min \left[\omega_{ss}, \cos^{-1} \left(\frac{-xy - \sqrt{x^2 - y^2 + 1}}{x^2 + 1} \right) \right] \quad (18)$$

where:

$$x = \frac{\cos \phi}{\sin \gamma_c \tan \beta} + \frac{\sin \phi}{\tan \gamma_c} \quad (19)$$

$$y = \tan \delta \left(\frac{\sin \phi}{\sin \gamma_c \tan \beta} - \frac{\cos \phi}{\tan \gamma_c} \right) \quad (20)$$

The zenith angles at sunrise and sunset z_{cr} , z_{cs} on the surface is given by Eqs. (5) and (15) to (20).

For summer $|\omega_{sr}| \geq |\omega_{cr}|$, and $\omega_{ss} \geq \omega_{cs}$; and for winter $|\omega_{sr}| \leq |\omega_{cr}|$, and $\omega_{ss} \leq \omega_{cs}$ for a surface oriented toward the equator. Therefore, the actual sunrise or sunset hour angles on an inclined surface are determined by finding the minima:

$$\omega_{cr} = \min \{ |\omega_{sr}|, |\omega_{cr}| \} \quad (21)$$

$$\omega_{cs} = \min \{ \omega_{ss}, \omega_{cs} \} \quad (22)$$

respectively.

2.3 Solar Angles of a Vertical Surface

The Sun angle of incidence on a vertical surface, is given by Eq. (13) or (14) for $\beta = 90^\circ$, i.e.,

$$\cos \theta = \sin z (\cos \gamma_s \cos \gamma_c + \sin \gamma_s \sin \gamma_c) \quad (23)$$

$$\cos \theta = (\sin \phi \cos \delta \cos \omega - \cos \phi \sin \delta) \cos \gamma_c + \cos \delta \sin \omega \sin \gamma_c \quad (24)$$

The sunrise and sunset hour angles on the surface are given by Eqs. (15) to (20), where now:

$$x = \frac{\sin \phi}{\tan \gamma_s} \quad (25)$$

$$y = -\tan \delta \frac{\cos \phi}{\tan \gamma_c} \quad (26)$$

2.4 Surface Facing the Equator

The Sun angle of incidence on an inclined surface β , facing the equator ($\gamma_c = 0$) is given by:

$$\cos \theta = \cos \beta \cos z + \sin \beta \sin z \cos \gamma_s \quad (27)$$

or

$$\cos \theta = \sin \delta \sin(\phi - \beta) + \cos \delta \cos(\phi - \beta) \cos \omega \quad (28)$$

For the particular case of $\beta = \phi$ we have:

$$\cos \theta = \cos \delta \cos \omega \quad (29)$$

The sunrise ω_{cr} and sunset ω_{cs} hour angles on the inclined surface facing the equator are:

$$\omega_{cr} = -\cos^{-1}[-\tan \delta \tan(\phi - \beta)] \quad (30)$$

$$\omega_{cs} = \cos^{-1}[-\tan \delta \tan(\phi - \beta)] \quad (31)$$

3. OPTIMAL ANGLES

3.1 Clear Skies

For clear days, the solar irradiance is symmetrical around noon and is maximum at true solar noon, $\omega = 0$.

The optimal angles γ_c and β of the surface may be determined based on the direct beam irradiance at noon for a clear day, i.e., results that are obtained from the differentiation of Eq. (14) with respect to γ_c and β at $\omega = 0$. The optimal azimuth of the surface is therefore:

$$\gamma_c = 0 \quad (32)$$

i.e., the surface is facing south in the northern hemisphere, or facing north in the southern hemisphere.

The optimal inclination angle is:

$$\beta = \phi - \delta \quad (33)$$

i.e., the surface is normal to the Sun rays at solar noon.

The solar incidence angle becomes (Eq. (28)):

$$\cos \theta = \sin^2 \delta + \cos^2 \delta \cos \omega \quad (34)$$

The solar declination angle varies daily, and for a stationary surface an average declination angle δ is used. Equation (33) thus becomes:

$$\beta_p = \phi - \delta_p \quad (35)$$

where δ_p is the average declination angle for a given period p , and β_p is the optimal inclination angle for that period. The yearly average declination angle is $\delta_p = 0$ and Eq. (35) becomes:

$$\beta_y = \phi \quad (36)$$

Substituting $\beta = \phi$ in Eq. (28), the angle of incidence becomes:

$$\cos \theta = \cos \delta \cos \omega \quad (37)$$

A better approximation for the optimal angles γ_c and β of the surface is obtained based on the daily beam insolation on the surface from sunrise to sunset, i.e., $\int_{-\omega_{cr}}^{\omega_{cs}} G_b \cos \theta d\omega$. A clear day is assumed for the calculation, symmetrical around noon, and with a sinusoidal variation of the beam irradiance.

Differentiation of the daily beam insolation with respect to γ_c and β we obtain:

$$\gamma_c = 0 \quad (38)$$

and

$$\tan \beta = \frac{\cos \omega_{cr} \sin \phi \cos \delta - [1 - (2\omega_{cr}/\pi)^2] \cos \phi \sin \delta}{\cos \omega_{cr} \cos \phi \cos \delta + [1 + (2\omega_{cr}/\pi)^2] \sin \phi \sin \delta} \quad (39)$$

where ω_{cr} is given by Eq. (30). For winter

$$\min \{|\omega_{sr}|, |\omega_{cr}|\} = \omega_{sr}$$

The Sun hour angle ω_{cr} on the surface is by itself a function of β , and since the optimal inclination angle β for summer is small, we may replace ω_{cr} by ω_{sr} (Eqs. (8) and (30)). Equation (39) may now be written as:

$$\tan \beta = \frac{\cos \omega_{sr} \sin \phi \cos \delta - [1 - (2\omega_{sr}/\pi)^2] \cos \phi \sin \delta}{\cos \omega_{sr} \sin \phi \cos \delta + [1 + (2\omega_{sr}/\pi)^2] \cos \phi \sin \delta} \quad (40)$$

3.2 Cloudy Skies

For days with high optical depth ("cloudy" skies) or days with appreciable diffuse irradiance, the surface optimal inclination angle may be determined by all three components of the solar irradiance. The daily global insolation, H_β , in $\text{Whr}/\text{m}^2\text{-day}$ is given (see Eq. (3)) by:

$$H_\beta = \frac{12.33}{\pi} \int_{\omega_{cr}}^{\omega_{cs}} [G_b \cos \theta + G_{dh} \cos^2(\beta/2) + a_l G_h \sin^2(\beta/2)] d\omega \quad (41)$$

The daily global insolation may also be given as a summation, i.e.,

$$H_\beta = \frac{12.33}{\pi} \left\{ \sum_{\omega_{cr}}^{\omega_{cs}} G_{bi} \cos \theta_i \Delta\omega + \sum_{\omega_{sr}}^{\omega_{ss}} [G_{dhi} \cos^2(\beta/2) + al G_{hi} \sin^2(\beta/2)] \Delta\omega \right\} \quad (42)$$

where the subscript i corresponds to the irradiance at hour angle ω_i and $\Delta\omega$ is the solar angle interval.

The factor 12.33 accounts for the 24.66 hr Mars day; for Earth, this factor is exactly 12.

In this section we will determine the surface optimal inclination angle for stationary surfaces. For isotropic skies, the optimal azimuth angle is at $\gamma_c = 0$ and the solar incidence angle θ is given by Eq. (28). The optimal inclination angle is obtained from the differentiation of Eq. (42) with respect to β . The hour angles ω_{cr} and ω_{cs} depend on β (see Eqs. (30) and (31)), therefore, the evaluation of the derivative becomes complicated. However, as a good approximation, ω_{cr} and ω_{cs} may be replaced by ω_{sr} and ω_{ss} , respectively. The optimal β is obtained from:

$$\frac{\partial H_\beta}{\partial \beta} = \sum_{\omega_{sr}}^{\omega_{ss}} G_{bi} \frac{\partial(\cos \theta_i)}{\partial \beta} \Delta\omega + \frac{1}{2} \sin \beta \sum_{\omega_{sr}}^{\omega_{ss}} (al G_{hi} - G_{dhi}) \Delta\omega = 0$$

and by using Eq. (28), the daily optimal inclination angle becomes:

$$\tan \beta = \frac{\sin \phi \cos \delta \sum_{\omega_{sr}}^{\omega_{ss}} G_{bi} \cos \omega_i \Delta\omega - \cos \phi \sin \delta \sum_{\omega_{sr}}^{\omega_{ss}} G_{bi} \Delta\omega}{\frac{1}{2} \sum_{\omega_{sr}}^{\omega_{ss}} (G_{dhi} - al G_{hi}) \Delta\omega + \sin \phi \sin \delta \sum_{\omega_{sr}}^{\omega_{ss}} G_{bi} \Delta\omega + \cos \phi \cos \delta \sum_{\omega_{sr}}^{\omega_{ss}} G_{bi} \cos \omega_i \Delta\omega} \quad (43)$$

4. SOLAR RADIATION ON AN INCLINED STATIONARY SURFACE

The calculation of the solar irradiance on an inclined surface is based on the beam irradiance G_b , and on the global and diffuse irradiances G_h and G_{dh} on a horizontal surface, respectively, as given by Eq. (3). These irradiances for Mars were derived in Ref. [1]. The daily global insolation on an inclined surface with an angle β is obtained by integrating the irradiance over the period from sunrise to sunset, or may be written as a summation as:

$$H_{\beta} = \sum_{\omega_{cr}}^{\omega_{cs}} G_{bi} \cos \theta_i \Delta\omega + \sum_{\omega_{sr}}^{\omega_{ss}} \left[G_{dhi} \cos^2(\beta/2) + a_l G_{hi} \sin^2(\beta/2) \right] \Delta\omega \quad (44)$$

where the subscript i corresponds to the irradiance at solar angle ω_i , and $\Delta\omega$ is the solar angle interval. The sunrise ω_{sr} and sunset ω_{ss} hour angles, and the sunrise ω_{cr} and sunset ω_{cs} hour angles on an inclined surface are given in Eqs. (8), (9), and (15) to (22), respectively. The angle of incidence θ is a function of the surface azimuth γ_c and inclination β angles.

4.1 Surface Facing the Equator

The optimal surface inclination angle may be determined for clear skies based on the beam irradiance (or daily beam insolation), or based on the daily global insolation. The yearly optimal inclination angle of a surface is given by Eq. (36), i.e.,

$$\beta_y = \phi \quad (45)$$

and the Sun incident angle is given by Eq. (37), i.e.,

$$\cos \theta = \cos \delta \cos \omega \quad (46)$$

The sunrise hour angle ω_{cr} on the inclined surface is needed for Eq. (43) to calculate the daily beam insolation on the surface. Table I gives the sunrise time on a surface for $\beta = \phi$ using Eq. (30) for different latitudes in the range between $\phi = -90^\circ$ to 90° , and for different areocentric longitudes between $L_s = 0^\circ$ to 360° . These times are in terms of actual (terrestrial) hours (hr), rather than Mars hours. Note that the sunrise time on a inclined surface is defined as the time in hours (referenced to midnight = 0) when the Sun is first visible from the front surface. This is not necessarily the time that the Sun rises over the horizon. These times are only the same during the local autumn and winter. During spring and summer, the Sun illuminates the back side of the surface before $\omega = -90^\circ$ (6.16 hr) and after $\omega = +90^\circ$ (18.49 hr). The sunrise hour angle on the surface is then determined by Eq. (21). The times 6.00 and 12.00 in Table I for high latitudes indicate polar days and polar nights, respectively. Table II gives the daily global insolation H for a Martian year for $\beta = \phi$ in kWhr/m²-day at Viking Landers locations VLI($\phi = 22.3^\circ$ N) and VL2($\phi = 47.7^\circ$ N) for the measured opacities. The insolation is broken down into

the beam H_b , diffuse H_d and albedo H_{al} components. The variation of the global insolation is also shown in Fig. 5. The difference in the daily insolation between a horizontal and an inclined surface for $\beta = \phi$ at VL1 and VL2 is shown in Fig. 6 as a percentage gain (or loss) compared to the horizontal surface [1]. Figure 7 shows the insolation at VL1 and VL2 on an inclined surface, $\beta = \phi$, for clear skies with $\tau = 0.5$. The effect of the global storms can be noticed by comparing Figs. 5 and 7.

The variation of the global insolation for the entire planet for inclined surfaces, $\beta = \phi$, at local latitudes may be of interest. For this purpose we resort to the optical depth model $\tau(\phi, L_g)$ [1, Eq. (1)]. The results are shown in Fig. 8. It is also interesting to know the insolation for the entire planet for clear skies throughout the year. Figure 9 shows the insolation on inclined surfaces, $\beta = \phi$, at local latitudes for $\tau = 0.5$.

The optimal inclination angle of a surface will now be determined based on the insolation rather than on the irradiance using Eq. (43). The yearly optimal inclination angle resulted in 6.5° at VL1 and 22° at VL2 for the measured opacities. Table III gives the daily direct beam, diffuse and the albedo components as well as the daily global insolation for the optimal inclination angles at VL1 and VL2. By comparing Tables II and III we obtain the percentage gain in the yearly insolation for the two installations: the approximate ($\beta = \phi$) and the exact optimal angles. The gain in the yearly global insolation is 2.47 percent at VL1 and 6.46 percent at VL2 in favor of the exact inclination angle.

4.2 Vertical Surface

A special case is a vertical surface, i.e., $\beta = 90^\circ$. A vertical bifacial surface (two-sided surface) acting as a PV array or as a radiator may be of special interest. The variation of the daily global insolation on a bifacial vertical surface is therefore calculated at different azimuth angles γ_c at VL1 for the observed opacities, and is shown in Fig. 10. The azimuth $\gamma_c = 0$ indicates that side A is facing south and side B is toward north. The figure shows that there is a small difference in the insolation for different azimuth angles at times with dust storms since the insolation is dictated mainly by the diffuse light, however, for clear skies the azimuth effects the global insolation. The best orientation for a PV array to face would be the east-west direction, and for a radiator the north-south direction.

5. DISCUSSION

In addition to the sunlight availability, operational considerations for Mars photovoltaic power systems include the low operating temperature [3], wind [3], dust, and the chemical environment of Mars. These are considered in Ref. [4] along with a discussion of the merits of various types of solar cells which may be used for power systems on Mars.

The low operating temperatures will increase the cell conversion efficiency by a greater amount for cells with a higher temperature coefficient, and thus reduce the advantage in efficiency of GaAs solar cells over silicon. For example, at an operating temperature of 200 K (the peak daytime temperature at the VL1 site during the 1977b dust storm [3]), the power output of a silicon cell will increase by nearly 45 percent; while a GaAs cell will only increase by 20 percent.

The temperature cycling of the arrays during the Mars day/night cycle is also a consideration for array lifetimes. The temperature encountered is similar to the temperature extremes encountered by a solar array in geosynchronous orbit (GEO) during eclipse, but the cycle time is considerably slower (e.g., cooling from peak temperature to minimum temperature in about 12 hr on Mars, versus 1 hr in GEO). It is thus expected that an array designed to survive the temperature cycling environment of GEO should also survive Mars conditions.

The sunlight is also spectrally shifted (reddened) due to dust. The peak of the atmospheric transmission is about $0.8 \mu\text{m}$ [5], and the amount of variation between peak and average transmission increases with atmospheric opacity and with zenith angle. This peak transmission is close to the peak spectral response wavelength of both silicon solar and GaAs cells, resulting in a slight increase in conversion efficiency [6].

Dust accumulation on the cells by settling from the atmosphere may be a significant problem for long duration missions without a mechanism for clearing dust from the arrays. The dust deposition rate is estimated to result in an average decrease of 20 to 80 percent from initial power levels over the course of one Mars year [7], depending on the number of dust storms. Actual arrays at a given location may have

higher or lower amounts of obscuration, however, since the dust settling rate is believed to be strongly dependant on location. There may be removal of dust by wind as well as deposition. Although the Viking lander did not measure winds high enough to remove deposited dust, views from the Viking cameras showed a gradual darkening of the bright dust layers deposited on the surface following global storms, indicative of dust removal.

Several dust removal mechanisms can be envisioned. It may be desirable to design arrays with surfaces that can be raised to “flap” in the wind to shake dust free, or else arrays with naturally flexible surfaces. Alternately, an array surface which can be charged alternately to a large positive and then negative potential to remove dust by electrostatic repulsion is a possibility.

Finally, this analysis has discussed the total insolation over the course of a Mars day. For many applications, it is also useful to make the power profile during the day as flat as possible, in order to minimize the requirements for storage. In particular, it is important to maximize the power production near sunrise and sunset. One method to accomplish this with a fixed array is with the use of a “tent” array, with surface elements tilted toward the east and to the west [8]. This reduces the total insolation produced over the day, but increases the direct beam component of the insolation in the early morning and late evening. Thus, this is most effective in flattening the power profile for low optical depths.

6. REFERENCES

- [1] J. Appelbaum, G.A. Landis, and I. Sherman, "Solar Radiation on Mars—Update 1991," *Solar Energy*, Vol. 50, No. 1, 1993, pp. 35–51.
- [2] M. Iqbal, *An Introduction to Solar Radiation*, Academic Press, 1983.
- [3] R.W. Zurek, J.R. Barnes, R.M. Haberle, J.B. Pollack, J.E. Tillman, and C.B. Leovy, "Dynamics of the Atmosphere of Mars," *Mars*, University of Arizona Press, Tucson, AZ, 1992, pp. 835–933.
- [4] G.A. Landis and J. Appelbaum, "Photovoltaic Power Options for Mars," *Space Power*, Vol. 10, No. 2, 1991, pp. 225–237.
- [5] R.M. Haberle, et al., "Atmospheric Effects on the Utility of Solar Power on Mars," *Resources of Near Earth Space*, University of Arizona Press, to be published.
- [6] D. Burger, "Solar Array Corrections for the Mars Surface," in *Case for Mars V*, Boulder, CO, May 1993, pp. 26–29.
- [7] G.A. Landis, "Instrumentation for Measurement of Dust Deposition on Solar Arrays on Mars," in *Case for Mars V*, Boulder, CO, May 1993, pp. 26–29.
- [8] G.A. Landis, S.G. Bailey, D.J. Brinker, and D.J. Flood, "Photovoltaic Power for a Lunar Base," *Acta Astronautica*, Vol. 22, 1990, pp. 197–203.

Table I.—Sunrise solar time on an inclined surface $\beta = \phi$

Ls	LATITUDE, ϕ , deg.																		
	-90	-80	-70	-60	-50	-40	-30	-20	-10	0	10	20	30	40	50	60	70	80	90
0	6.00	6.00	6.00	6.00	6.00	6.00	6.00	6.00	6.00	6.00	6.00	6.00	6.00	6.00	6.00	6.00	6.00	6.00	6.00
5	12.00	6.80	6.39	6.24	6.17	6.12	6.08	6.05	6.02	6.00	6.00	6.00	6.00	6.00	6.00	6.00	6.00	6.00	6.00
10	12.00	7.64	6.78	6.49	6.33	6.24	6.16	6.10	6.05	6.00	6.00	6.00	6.00	6.00	6.00	6.00	6.00	6.00	6.00
15	12.00	8.57	7.17	6.73	6.50	6.35	6.24	6.15	6.07	6.00	6.00	6.00	6.00	6.00	6.00	6.00	6.00	6.00	6.00
20	12.00	9.72	7.57	6.97	6.67	6.47	6.32	6.20	6.10	6.00	6.00	6.00	6.00	6.00	6.00	6.00	6.00	6.00	6.00
25	12.00	12.00	7.99	7.22	6.83	6.58	6.40	6.25	6.12	6.00	6.00	6.00	6.00	6.00	6.00	6.00	6.00	6.00	6.00
30	12.00	12.00	8.42	7.46	6.99	6.70	6.48	6.30	6.15	6.00	6.00	6.00	6.00	6.00	6.00	6.00	6.00	6.00	6.00
35	12.00	12.00	8.88	7.70	7.15	6.80	6.55	6.35	6.17	6.00	6.00	6.00	6.00	6.00	6.00	6.00	6.00	6.00	6.00
40	12.00	12.00	9.38	7.95	7.31	6.91	6.62	6.39	6.19	6.00	6.00	6.00	6.00	6.00	6.00	6.00	6.00	6.00	6.00
45	12.00	12.00	9.94	8.18	7.46	7.01	6.69	6.44	6.21	6.00	6.00	6.00	6.00	6.00	6.00	6.00	6.00	6.00	6.00
50	12.00	12.00	10.64	8.42	7.60	7.11	6.76	6.48	6.23	6.00	6.00	6.00	6.00	6.00	6.00	6.00	6.00	6.00	6.00
55	12.00	12.00	12.00	8.64	7.73	7.20	6.82	6.51	6.25	6.00	6.00	6.00	6.00	6.00	6.00	6.00	6.00	6.00	6.00
60	12.00	12.00	12.00	8.85	7.86	7.28	6.87	6.55	6.26	6.00	6.00	6.00	6.00	6.00	6.00	6.00	6.00	6.00	6.00
65	12.00	12.00	12.00	9.05	7.97	7.35	6.92	6.58	6.28	6.00	6.00	6.00	6.00	6.00	6.00	6.00	6.00	6.00	6.00
70	12.00	12.00	12.00	9.22	8.06	7.42	6.96	6.60	6.29	6.00	6.00	6.00	6.00	6.00	6.00	6.00	6.00	6.00	6.00
75	12.00	12.00	12.00	9.37	8.14	7.46	6.99	6.62	6.30	6.00	6.00	6.00	6.00	6.00	6.00	6.00	6.00	6.00	6.00
80	12.00	12.00	12.00	9.48	8.20	7.50	7.02	6.64	6.31	6.00	6.00	6.00	6.00	6.00	6.00	6.00	6.00	6.00	6.00
85	12.00	12.00	12.00	9.55	8.23	7.52	7.03	6.65	6.31	6.00	6.00	6.00	6.00	6.00	6.00	6.00	6.00	6.00	6.00
90	12.00	12.00	12.00	9.58	8.24	7.53	7.04	6.65	6.31	6.00	6.00	6.00	6.00	6.00	6.00	6.00	6.00	6.00	6.00
95	12.00	12.00	12.00	9.55	8.23	7.52	7.03	6.65	6.31	6.00	6.00	6.00	6.00	6.00	6.00	6.00	6.00	6.00	6.00
100	12.00	12.00	12.00	9.48	8.20	7.50	7.02	6.64	6.31	6.00	6.00	6.00	6.00	6.00	6.00	6.00	6.00	6.00	6.00
105	12.00	12.00	12.00	9.37	8.14	7.46	6.99	6.62	6.30	6.00	6.00	6.00	6.00	6.00	6.00	6.00	6.00	6.00	6.00
110	12.00	12.00	12.00	9.22	8.06	7.42	6.96	6.60	6.29	6.00	6.00	6.00	6.00	6.00	6.00	6.00	6.00	6.00	6.00
115	12.00	12.00	12.00	9.05	7.97	7.35	6.92	6.58	6.28	6.00	6.00	6.00	6.00	6.00	6.00	6.00	6.00	6.00	6.00
120	12.00	12.00	12.00	8.85	7.86	7.28	6.87	6.55	6.26	6.00	6.00	6.00	6.00	6.00	6.00	6.00	6.00	6.00	6.00
125	12.00	12.00	12.00	8.64	7.73	7.20	6.82	6.51	6.25	6.00	6.00	6.00	6.00	6.00	6.00	6.00	6.00	6.00	6.00
130	12.00	12.00	10.64	8.42	7.60	7.11	6.76	6.48	6.23	6.00	6.00	6.00	6.00	6.00	6.00	6.00	6.00	6.00	6.00
135	12.00	12.00	9.94	8.18	7.46	7.01	6.69	6.44	6.21	6.00	6.00	6.00	6.00	6.00	6.00	6.00	6.00	6.00	6.00
140	12.00	12.00	9.38	7.95	7.31	6.91	6.62	6.39	6.19	6.00	6.00	6.00	6.00	6.00	6.00	6.00	6.00	6.00	6.00
145	12.00	12.00	8.88	7.70	7.15	6.80	6.55	6.35	6.17	6.00	6.00	6.00	6.00	6.00	6.00	6.00	6.00	6.00	6.00
150	12.00	12.00	8.42	7.46	6.99	6.70	6.48	6.30	6.15	6.00	6.00	6.00	6.00	6.00	6.00	6.00	6.00	6.00	6.00
155	12.00	12.00	7.99	7.22	6.83	6.58	6.40	6.25	6.12	6.00	6.00	6.00	6.00	6.00	6.00	6.00	6.00	6.00	6.00
160	12.00	9.72	7.57	6.97	6.67	6.47	6.32	6.20	6.10	6.00	6.00	6.00	6.00	6.00	6.00	6.00	6.00	6.00	6.00
165	12.00	8.57	7.17	6.73	6.50	6.35	6.24	6.15	6.07	6.00	6.00	6.00	6.00	6.00	6.00	6.00	6.00	6.00	6.00
170	12.00	7.64	6.78	6.49	6.33	6.24	6.16	6.10	6.05	6.00	6.00	6.00	6.00	6.00	6.00	6.00	6.00	6.00	6.00
175	12.00	6.80	6.39	6.24	6.17	6.12	6.08	6.05	6.02	6.00	6.00	6.00	6.00	6.00	6.00	6.00	6.00	6.00	6.00
180	6.00	6.00	6.00	6.00	6.00	6.00	6.00	6.00	6.00	6.00	6.00	6.00	6.00	6.00	6.00	6.00	6.00	6.00	6.00
185	6.00	6.00	6.00	6.00	6.00	6.00	6.00	6.00	6.00	6.00	6.02	6.05	6.08	6.12	6.17	6.24	6.39	6.80	12.00
190	6.00	6.00	6.00	6.00	6.00	6.00	6.00	6.00	6.00	6.00	6.05	6.10	6.16	6.24	6.33	6.49	6.78	7.64	12.00
195	6.00	6.00	6.00	6.00	6.00	6.00	6.00	6.00	6.00	6.00	6.07	6.15	6.24	6.35	6.50	6.73	7.17	8.57	12.00
200	6.00	6.00	6.00	6.00	6.00	6.00	6.00	6.00	6.00	6.00	6.10	6.20	6.32	6.47	6.67	6.97	7.57	9.72	12.00
205	6.00	6.00	6.00	6.00	6.00	6.00	6.00	6.00	6.00	6.00	6.12	6.25	6.40	6.58	6.83	7.22	7.99	12.00	12.00
210	6.00	6.00	6.00	6.00	6.00	6.00	6.00	6.00	6.00	6.00	6.15	6.30	6.48	6.70	6.99	7.46	8.42	12.00	12.00
215	6.00	6.00	6.00	6.00	6.00	6.00	6.00	6.00	6.00	6.00	6.17	6.35	6.55	6.80	7.15	7.70	8.88	12.00	12.00
220	6.00	6.00	6.00	6.00	6.00	6.00	6.00	6.00	6.00	6.00	6.19	6.39	6.62	6.91	7.31	7.95	9.38	12.00	12.00
225	6.00	6.00	6.00	6.00	6.00	6.00	6.00	6.00	6.00	6.00	6.21	6.44	6.69	7.01	7.46	8.18	9.94	12.00	12.00
230	6.00	6.00	6.00	6.00	6.00	6.00	6.00	6.00	6.00	6.00	6.23	6.48	6.76	7.11	7.60	8.42	10.64	12.00	12.00
235	6.00	6.00	6.00	6.00	6.00	6.00	6.00	6.00	6.00	6.00	6.25	6.51	6.82	7.20	7.73	8.64	12.00	12.00	12.00
240	6.00	6.00	6.00	6.00	6.00	6.00	6.00	6.00	6.00	6.00	6.26	6.55	6.87	7.28	7.86	8.85	12.00	12.00	12.00
245	6.00	6.00	6.00	6.00	6.00	6.00	6.00	6.00	6.00	6.00	6.28	6.58	6.92	7.35	7.97	9.05	12.00	12.00	12.00
250	6.00	6.00	6.00	6.00	6.00	6.00	6.00	6.00	6.00	6.00	6.29	6.60	6.96	7.42	8.06	9.22	12.00	12.00	12.00
255	6.00	6.00	6.00	6.00	6.00	6.00	6.00	6.00	6.00	6.00	6.30	6.62	6.99	7.46	8.14	9.37	12.00	12.00	12.00
260	6.00	6.00	6.00	6.00	6.00	6.00	6.00	6.00	6.00	6.00	6.31	6.64	7.02	7.50	8.20	9.48	12.00	12.00	12.00
265	6.00	6.00	6.00	6.00	6.00	6.00	6.00	6.00	6.00	6.00	6.31	6.65	7.03	7.52	8.23	9.55	12.00	12.00	12.00
270	6.00	6.00	6.00	6.00	6.00	6.00	6.00	6.00	6.00	6.00	6.31	6.65	7.04	7.53	8.24	9.58	12.00	12.00	12.00
275	6.00	6.00	6.00	6.00	6.00	6.00	6.00	6.00	6.00	6.00	6.31	6.65	7.03	7.52	8.23	9.55	12.00	12.00	12.00
280	6.00	6.00	6.00	6.00	6.00	6.00	6.00	6.00	6.00	6.00	6.31	6.64	7.02	7.50	8.20	9.48	12.00	12.00	12.00
285	6.00	6.00	6.00	6.00	6.00	6.00	6.00	6.00	6.00	6.00	6.30	6.62	6.99	7.46	8.14	9.37	12.00	12.00	12.00
290	6.00	6.00	6.00	6.00	6.00	6.00	6.00	6.00	6.00	6.00	6.29	6.60	6.96	7.42	8.06	9.22	12.00	12.00	12.00
295	6.00	6.00	6.00	6.00	6.00	6.00	6.00	6.00	6.00	6.00	6.28	6.58	6.92	7.35	7.97	9.05	12.00	12.00	12.00
300	6.00	6.00	6.00	6.00	6.00	6.00	6.00	6.00	6.00	6.00	6.26	6.55	6.87	7.28	7.86	8.85	12.00	12.00	12.00
305	6.00	6.00	6.00	6.00	6.00	6.00	6.00	6.00	6.00	6.00	6.25	6.51	6.82	7.20	7.73	8.64	12.00	12.00	12.00
310	6.00	6.00	6.00	6.00	6.00	6.00	6.00	6.00	6.00	6.00	6.23	6.48	6.76	7.11	7.60	8.42	10.64	12.00	12.00
315	6.00	6.00	6.00	6.00	6.00	6.00	6.00	6.00	6.00	6.00	6.21	6.44	6.69	7.01	7.46	8.18	9.94	12.00	12.00
320	6.00	6.00	6.00	6.00	6.00	6.00	6.00	6.00	6.00	6.00	6.19	6.39	6.62	6.91	7.31	7.95	9.38	12.00	12.00
325	6.0																		

Table II.—Daily insolation (global H , beam H_b , diffuse H_d , and albedo H_{al}) on an inclined surface for $\beta = \phi$ at VL1 and VL2

Ls	VL1				VL2			
	H	H _b	H _d	H _{al}	H	H _b	H _d	H _{al}
0	3355.0	1723.6	1604.5	26.9	2198.5	958.6	1160.1	79.8
5	3084.0	1247.0	1811.8	25.2	2628.9	1420.8	1116.3	91.8
10	3251.4	1513.4	1711.4	26.6	2909.2	1734.4	1073.9	100.9
15	3413.9	1829.2	1556.6	28.1	2565.5	1183.7	1285.5	96.3
20	3350.4	1705.0	1617.6	27.8	2872.2	1535.6	1230.0	106.6
25	3339.6	1692.1	1619.5	28.0	2787.6	1341.8	1338.5	107.3
30	3424.9	1901.7	1494.2	29.0	2918.2	1467.1	1337.6	113.5
35	3357.1	1767.1	1561.4	28.6	3260.4	1978.6	1155.6	126.2
40	3430.7	1980.6	1420.5	29.6	3361.8	2127.0	1102.4	132.4
45	3278.3	1625.4	1624.6	28.3	3312.9	1979.0	1200.1	133.8
50	3221.9	1513.2	1680.7	28.0	2919.9	1231.5	1566.2	122.2
55	3052.8	1177.2	1849.1	26.5	3353.0	1971.8	1240.6	140.6
60	3200.3	1485.0	1687.2	28.1	3370.6	1968.1	1259.0	143.5
65	3231.7	1565.4	1637.7	28.6	3387.8	1965.2	1276.4	146.2
70	3267.6	1656.9	1581.6	29.1	3455.0	2096.3	1207.5	151.2
75	3307.8	1757.3	1520.8	29.7	3471.3	2096.8	1221.1	153.4
80	3313.8	1755.8	1528.2	29.8	3395.8	1847.6	1398.0	150.2
85	3327.1	1760.2	1536.9	30.0	3509.8	2108.7	1244.3	156.8
90	3273.9	1566.0	1678.6	29.3	3532.3	2120.7	1253.6	158.0
95	3261.3	1485.7	1746.5	29.1	3557.0	2137.1	1261.0	158.9
100	3290.7	1501.7	1759.7	29.3	3487.2	1897.3	1435.6	154.3
105	3478.2	1944.3	1502.6	31.3	3511.2	1917.2	1439.6	154.4
110	3520.6	1973.9	1515.1	31.6	3534.5	1939.2	1441.2	154.1
115	3643.8	2273.0	1338.0	32.8	3723.5	2390.1	1172.1	161.3
120	3701.4	2318.9	1349.4	33.1	3872.3	2773.3	933.1	165.9
125	3761.4	2366.6	1361.4	33.4	3849.5	2633.6	1054.5	161.4
130	3822.7	2416.5	1372.5	33.7	3883.0	2674.7	1049.0	159.3
135	3884.5	2467.1	1383.5	33.9	3993.7	2913.3	920.6	159.8
140	3998.8	2684.4	1279.8	34.6	3852.2	2559.9	1141.2	151.1
145	3896.3	2260.5	1602.5	33.3	3955.8	2782.9	1022.5	150.4
150	3775.3	1903.6	1839.8	31.9	3861.6	2603.5	1114.3	143.8
155	3809.6	1930.3	1847.4	31.9	3850.2	2613.5	1097.3	139.4
160	3776.8	1832.7	1912.7	31.4	3950.3	2834.4	978.6	137.3
165	3794.3	1847.4	1915.6	31.3	3657.3	2395.0	1135.7	126.6
170	3739.8	1740.7	1968.5	30.6	3593.8	2365.8	1107.0	121.0
175	3735.8	1741.7	1963.8	30.3	2829.0	1376.8	1350.6	101.6
180	3721.1	1736.1	1955.0	30.0	2231.3	778.4	1368.1	84.8
185	3317.1	1159.8	2130.4	26.9	1868.8	505.0	1290.5	73.3
190	3104.8	934.7	2144.9	25.2	2094.9	798.2	1220.3	76.4
195	3161.0	1041.2	2094.3	25.5	2099.5	889.3	1136.6	73.6
200	3217.1	1161.3	2030.2	25.6	1797.1	657.4	1075.0	64.7
205	2372.6	328.6	2013.7	30.3	1130.4	162.6	915.7	52.1
210	1956.4	137.4	1789.5	29.5	855.4	49.9	752.4	53.1
215	2052.8	191.4	1830.9	30.5	816.2	60.4	710.6	45.2
220	2030.8	204.1	1798.0	28.7	739.4	52.3	647.2	39.9
225	2007.7	218.6	1762.1	27.0	685.5	51.5	599.2	34.8
230	2043.8	273.3	1745.9	24.6	877.5	207.3	637.0	33.2
235	2027.8	297.5	1707.4	22.9	625.5	70.7	528.9	25.9
240	2025.7	326.9	1677.3	21.5	520.5	35.2	461.2	24.1
245	2068.8	393.1	1656.0	19.7	629.0	117.9	486.6	24.5
250	2125.1	479.8	1627.4	17.9	529.1	70.8	436.8	21.5
255	2221.1	594.5	1609.2	17.4	406.4	21.3	366.7	18.4
260	2180.2	578.9	1584.2	17.1	401.6	26.2	358.2	17.2
265	1899.1	342.7	1538.3	18.1	442.4	49.5	374.7	18.2
270	1670.1	189.6	1460.4	20.1	335.7	7.8	310.3	17.6
275	1354.1	60.9	1272.7	20.5	307.6	2.8	285.7	19.1
280	1206.9	32.8	1155.8	18.3	300.1	1.5	278.0	20.6
285	1330.7	54.8	1255.8	20.1	321.1	2.6	297.5	21.0
290	1026.8	12.3	998.8	15.7	332.8	2.4	307.6	22.8
295	1167.7	24.5	1125.4	17.8	339.2	1.8	312.9	24.5
300	1260.6	36.0	1205.4	19.2	380.7	3.4	350.1	27.2
305	1451.5	71.1	1358.5	21.9	441.8	8.7	404.4	28.7
310	1728.7	160.8	1543.4	24.5	519.9	20.9	468.9	30.1
315	2052.7	357.6	1673.3	21.8	831.5	174.1	625.1	32.3
320	2250.1	504.1	1725.3	20.7	1201.4	449.2	711.0	41.2
325	2343.4	566.4	1756.2	20.8	1208.9	401.4	764.2	43.3
330	2479.9	679.3	1780.3	20.3	1331.7	458.7	825.3	47.7
335	2628.3	808.2	1799.1	21.0	1345.7	417.0	878.8	49.9
340	2581.6	726.0	1834.3	21.3	1076.1	154.7	870.0	51.4
345	3044.0	1281.2	1738.7	24.1	1645.4	578.4	1006.5	60.5
350	2908.0	1062.7	1821.9	23.4	1828.9	696.9	1065.3	66.7
355	3158.7	1403.9	1729.5	25.3	2243.0	1085.5	1079.5	78.0
360	3355.0	1723.6	1604.5	26.9	2198.5	958.6	1160.1	79.8
AVG	2841.0	1171.4	1643.2	26.3	2179.4	1153.0	937.9	88.5

Table III.—Daily insolation (global H , beam H_b , diffuse H_d , and albedo H_{al}) on optimal

inclined angles $\beta_{VL1} = 6.5^\circ$ and $\beta_{VL2} = 22^\circ$ at VL1 and VL2, respectively

VL1 beta optimal = 6.5°					VL2 beta optimal = 22.0°			
Ls	H	H _b	H _d	H _{al}	H	H _b	H _d	H _{al}
0	3322.7	1658.4	1662.0	2.3	2217.9	863.8	1336.3	17.8
5	3093.4	1214.9	1876.3	2.2	2614.6	1308.0	1286.2	20.4
10	3267.8	1493.4	1772.1	2.3	2891.9	1632.6	1236.8	22.5
15	3443.1	1829.1	1611.6	2.4	2638.6	1136.0	1481.2	21.4
20	3404.5	1725.7	1676.4	2.4	2948.4	1507.4	1417.3	23.7
25	3413.1	1733.6	1677.1	2.4	2908.4	1342.9	1541.6	23.9
30	3523.5	1973.7	1547.3	2.5	3066.1	1499.7	1541.1	25.3
35	3473.2	1854.4	1616.3	2.5	3434.3	2075.2	1331.0	28.1
40	3578.7	2104.8	1471.3	2.6	3580.1	2280.1	1270.5	29.5
45	3427.4	1741.6	1683.3	2.5	3570.0	2158.0	1382.2	29.8
50	3378.5	1635.7	1740.4	2.4	3182.0	1350.0	1804.8	27.2
55	3197.4	1280.4	1914.7	2.3	3684.7	2224.8	1428.6	31.3
60	3383.4	1633.5	1747.5	2.4	3735.8	2253.1	1450.7	32.0
65	3436.0	1737.2	1696.3	2.5	3782.2	2279.0	1470.6	32.6
70	3491.6	1850.8	1638.3	2.5	3889.1	2464.9	1390.5	33.7
75	3552.4	1974.5	1575.3	2.6	3927.9	2487.0	1406.8	34.1
80	3566.2	1980.4	1583.2	2.6	3836.9	2192.9	1610.5	33.5
85	3584.4	1989.5	1592.3	2.6	3995.1	2526.7	1433.5	34.9
90	3508.2	1766.6	1739.1	2.5	4023.9	2544.5	1444.2	35.2
95	3484.7	1672.9	1809.3	2.5	4048.9	2560.7	1452.8	35.4
100	3512.8	1687.4	1822.9	2.5	3940.2	2251.9	1653.9	34.4
105	3747.1	2187.8	1556.6	2.7	3954.3	2261.4	1658.5	34.4
110	3782.9	2210.7	1569.5	2.7	3961.8	2267.8	1659.7	34.3
115	3928.2	2539.3	1386.1	2.8	4174.1	2787.7	1350.5	35.9
120	3970.0	2569.4	1397.7	2.9	4325.5	3213.1	1075.5	36.9
125	4011.7	2599.4	1409.4	2.9	4245.9	2996.0	1214.0	35.9
130	4052.8	2628.8	1421.1	2.9	4236.1	2991.3	1209.3	35.5
135	4093.4	2656.5	1434.0	2.9	4305.0	3209.3	1060.1	35.6
140	4190.7	2862.0	1325.7	3.0	4099.2	2750.2	1315.3	33.7
145	4037.4	2375.6	1658.9	2.9	4147.5	2936.4	1177.6	33.5
150	3881.4	1973.5	1905.1	2.8	3999.3	2683.2	1284.1	32.0
155	3893.5	1977.6	1913.1	2.8	3930.0	2635.5	1263.5	31.0
160	3839.2	1854.4	1982.1	2.7	3957.7	2799.1	1128.0	30.6
165	3832.4	1846.4	1983.3	2.7	3644.3	2307.3	1308.8	28.2
170	3758.7	1717.8	2038.3	2.6	3530.8	2228.9	1275.0	26.9
175	3733.6	1697.2	2033.8	2.6	2845.8	1267.1	1556.1	22.6
180	3698.1	1670.4	2025.1	2.6	2296.1	701.4	1575.8	18.9
185	3310.8	1102.1	2206.4	2.3	1949.0	445.9	1486.8	16.3
190	3100.8	877.6	2221.0	2.2	2113.2	690.1	1406.1	17.0
195	3136.4	965.4	2168.8	2.2	2078.5	752.9	1309.2	16.4
200	3167.3	1063.4	2101.7	2.2	1798.5	545.6	1238.5	14.4
205	2386.8	298.1	2086.1	2.6	1199.5	132.7	1055.2	11.6
210	1979.2	123.4	1853.2	2.6	918.5	40.0	866.7	11.8
215	2068.6	169.9	1896.1	2.6	876.6	47.5	819.0	10.1
220	2043.5	179.2	1861.8	2.5	794.5	40.4	745.2	8.9
225	2017.0	189.9	1824.8	2.3	737.1	39.0	690.4	7.7
230	2045.6	235.0	1808.5	2.1	895.1	154.0	733.7	7.4
235	2023.7	253.4	1768.3	2.0	667.0	51.8	609.4	5.8
240	2014.5	276.0	1736.6	1.9	562.1	25.5	531.2	5.4
245	2045.4	329.2	1714.5	1.7	650.0	84.0	560.6	5.4
250	2085.6	398.9	1685.2	1.5	557.8	49.9	503.1	4.8
255	2159.3	491.2	1666.6	1.5	441.6	14.9	422.6	4.1
260	2118.9	476.6	1640.8	1.5	434.9	18.2	412.9	3.8
265	1876.8	282.1	1593.1	1.6	470.1	34.3	431.7	4.1
270	1670.4	156.3	1512.4	1.7	366.7	5.4	357.4	3.9
275	1370.3	50.4	1318.1	1.8	335.3	1.9	329.1	4.3
280	1225.8	27.2	1197.0	1.6	326.0	1.1	320.3	4.6
285	1347.7	45.6	1300.4	1.7	349.4	1.9	342.8	4.7
290	1046.0	10.3	1034.3	1.4	361.1	1.7	354.3	5.1
295	1187.4	20.6	1165.3	1.5	367.3	1.3	360.5	5.5
300	1280.3	30.5	1248.1	1.7	411.8	2.5	403.2	6.1
305	1469.7	60.8	1407.0	1.9	478.8	6.4	466.0	6.4
310	1739.2	138.4	1598.7	2.1	562.4	15.6	540.1	6.7
315	2044.9	310.2	1732.8	1.9	859.0	131.6	720.2	7.2
320	2229.9	441.5	1786.6	1.8	1172.7	344.8	818.7	9.2
325	2322.0	501.5	1818.7	1.8	1204.4	314.1	880.7	9.6
330	2453.5	608.0	1843.7	1.8	1327.1	365.9	950.6	10.6
335	2597.5	731.7	1864.0	1.8	1363.3	339.4	1012.8	11.1
340	2566.2	665.3	1899.1	1.8	1142.5	128.8	1002.3	11.4
345	2989.8	1187.1	1800.6	2.1	1663.0	490.1	1159.4	13.5
350	2885.9	997.4	1886.5	2.0	1844.9	602.5	1227.5	14.9
355	3127.3	1333.8	1791.3	2.2	2218.8	957.7	1243.7	17.4
AVG	2911.5	1207.4	1701.8	2.3	2320.4	1220.2	1080.5	19.7

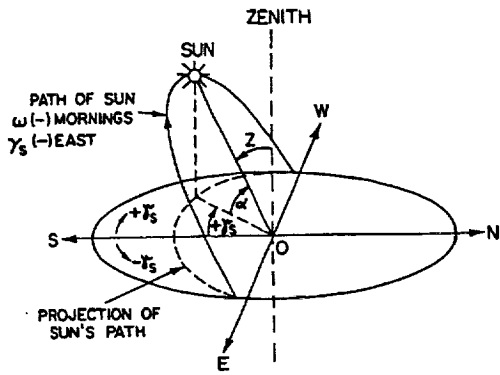


Figure 1.—Definition of angles for solar calculation.

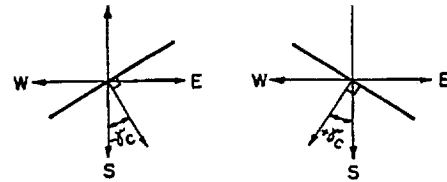


Figure 4.—Surface azimuth angle.

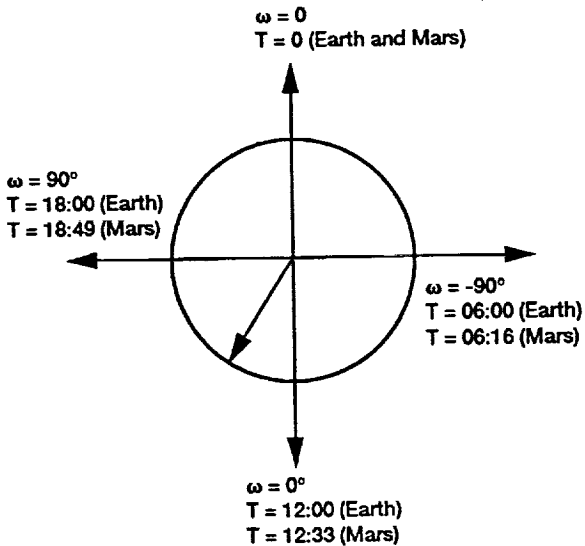


Figure 2.—Solar time and hour angle relation.

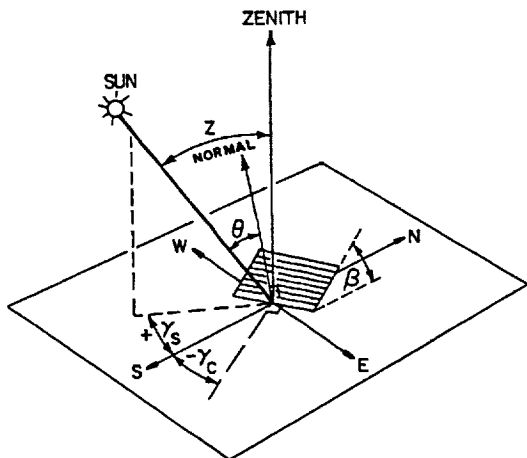


Figure 3.—Solar angles on an inclined surface.

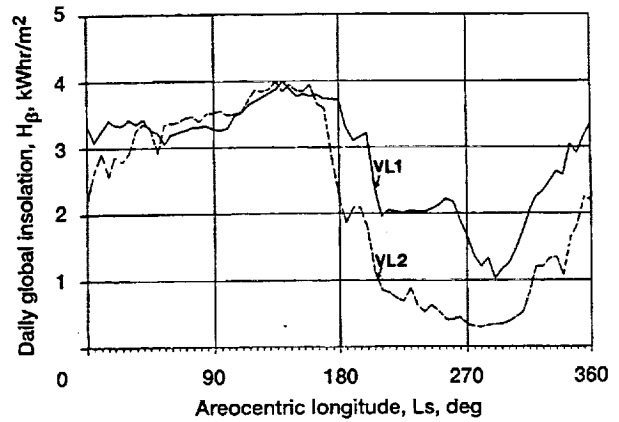


Figure 5.—Variation of daily global insolation on a tilted surface, $\beta = \phi$, at VL1 and VL2.

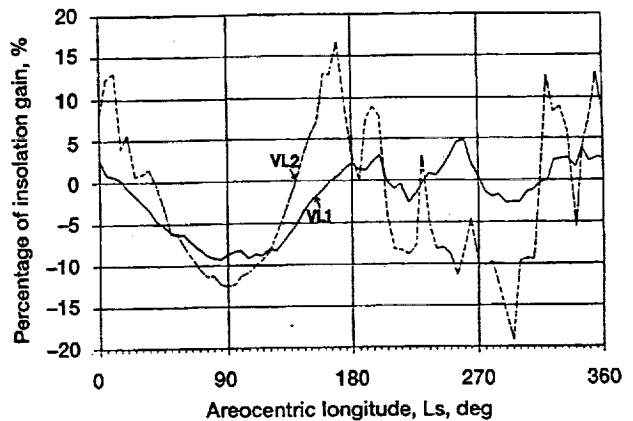


Figure 6.—Variation of daily global insolation loss (gain) on a tilted surface $\beta = \phi$ as compared to a horizontal surface at VL1 and VL2.

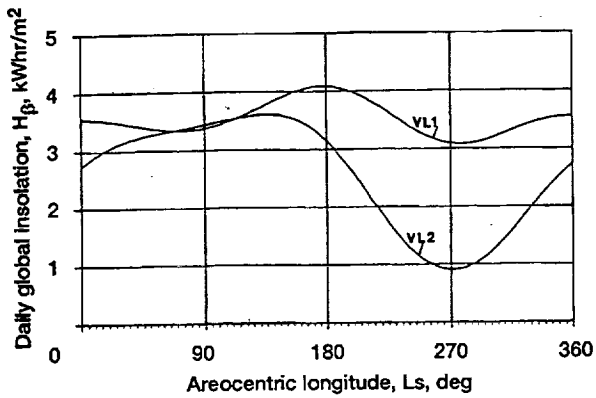


Figure 7.—Variation of daily global insolation on an inclined surface, $\beta = \phi$, at VL1 and VL2 for optical depth of 0.5.

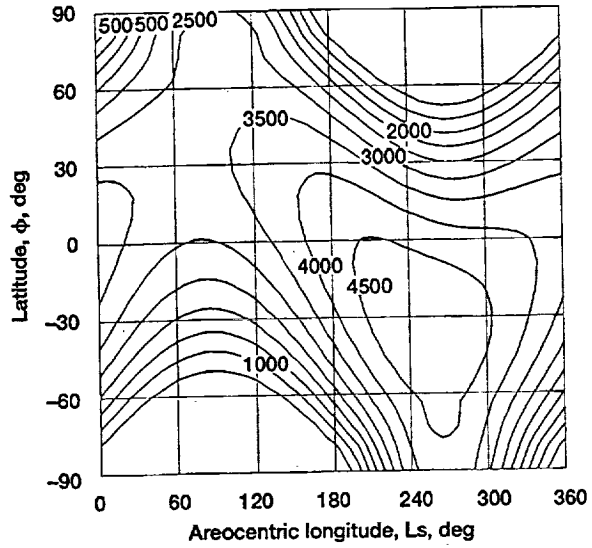


Figure 9.—Variation of daily global insolation H_{β} (kWhr/m²) with latitude and areocentric longitude on an inclined surface, $\beta = \phi$, for optical depth of 0.5.

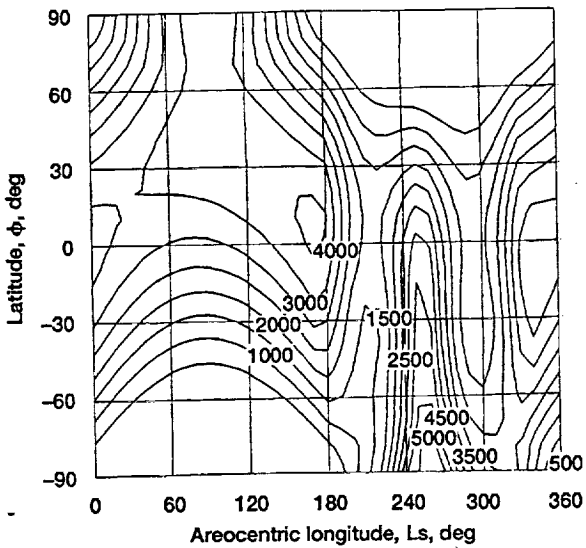


Figure 8.—Variation of daily global insolation H_{β} (kWhr/m²) with latitude and areocentric longitude on an inclined surface, $\beta = \phi$, based on the optical depth function [1, Eq. (1)].

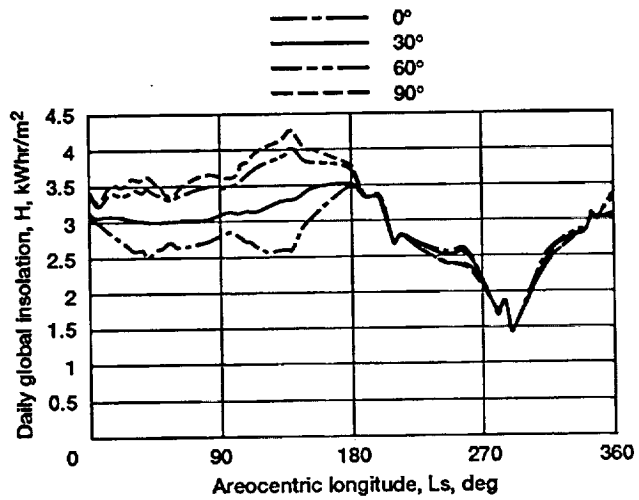


Figure 10.—Variation of daily global insolation on a bifacial vertical surface at different azimuth angle γ_c at VL1.

REPORT DOCUMENTATION PAGE

Form Approved
OMB No. 0704-0188

Public reporting burden for this collection of information is estimated to average 1 hour per response, including the time for reviewing instructions, searching existing data sources, gathering and maintaining the data needed, and completing and reviewing the collection of information. Send comments regarding this burden estimate or any other aspect of this collection of information, including suggestions for reducing this burden, to Washington Headquarters Services, Directorate for Information Operations and Reports, 1215 Jefferson Davis Highway, Suite 1204, Arlington, VA 22202-4302, and to the Office of Management and Budget, Paperwork Reduction Project (0704-0188), Washington, DC 20503.

1. AGENCY USE ONLY (Leave blank)	2. REPORT DATE October 1993	3. REPORT TYPE AND DATES COVERED Technical Memorandum	
4. TITLE AND SUBTITLE Solar Radiation on Mars: Stationary Photovoltaic Array		5. FUNDING NUMBERS WU-506-41-11	
6. AUTHOR(S) J. Appelbaum, I. Sherman and G.A. Landis		8. PERFORMING ORGANIZATION REPORT NUMBER E-8071	
7. PERFORMING ORGANIZATION NAME(S) AND ADDRESS(ES) National Aeronautics and Space Administration Lewis Research Center Cleveland, Ohio 44135-3191		10. SPONSORING/MONITORING AGENCY REPORT NUMBER NASA TM-106321	
9. SPONSORING/MONITORING AGENCY NAME(S) AND ADDRESS(ES) National Aeronautics and Space Administration Washington, D.C. 20546-0001		11. SUPPLEMENTARY NOTES J. Appelbaum, National Research Council NASA Research Associate on leave from Tel Aviv 69978 Israel (work funded by NASA Grant NAGW-2022); I. Sherman, Faculty of Engineering, Tel Aviv University, Ramat Aviv 69978, Israel; and G.A. Landis, Sverdrup Technology Inc., Lewis Research Center Group, 2001 Aerospace Parkway, Brook Park, Ohio 44142 (work funded NASA Contract NAS-33-25266). Responsible person, J. Appelbaum, (216) 433-2234.	
12a. DISTRIBUTION/AVAILABILITY STATEMENT Unclassified - Unlimited Subject Category 33		12b. DISTRIBUTION CODE	
13. ABSTRACT (Maximum 200 words) Solar energy is likely to be an important power source for surface-based operation on Mars. Photovoltaic cells offer many advantages. In this article we have presented analytical expressions and solar radiation data for stationary flat surfaces (horizontal and inclined) as a function of latitude, season and atmospheric dust load (optical depth). The diffuse component of the solar radiation on Mars can be significant, thus greatly affecting the optimal inclination angle of the photovoltaic surface.			
14. SUBJECT TERMS Mars; Optical depth; Photovoltaic array; Solar radiation; Solar angles; Optimal installation angles; Direct beam; Diffuse and albedo		15. NUMBER OF PAGES 21	
		16. PRICE CODE A03	
17. SECURITY CLASSIFICATION OF REPORT Unclassified	18. SECURITY CLASSIFICATION OF THIS PAGE Unclassified	19. SECURITY CLASSIFICATION OF ABSTRACT Unclassified	20. LIMITATION OF ABSTRACT